

# Implementing a Novel Highly Scalable Adaptive Photonic Beamformer using “Blind” Guided Accelerated Random Search

John Chang, *Member, IEEE*, James Meister, *Fellow, IEEE*, and Paul R. Prucnal, *Fellow, IEEE*

**Abstract**—A novel highly scalable adaptive photonic beamformer is proposed and experimentally verified. A single-mode-to-multimode combiner allows our system to recycle the same set of wavelengths for each antenna in the array. A “blind” search algorithm called the guided accelerated random search (GARS) algorithm is shown. A maximum cancellation of  $\sim 37$  dB is achieved within 50 iterations, while the presence of a signal of interest (SOI) is maintained. Cancellation across the 900 MHz and 2.4 GHz bands are shown to prove the broadband nature of the optical beamformer.

**Index Terms**—Adaptive arrays, beam steering, microwave photonics, optical signal processing, phased arrays.

## I. INTRODUCTION

WIRELESS communication has exploded in recent years, due to the emerging markets for mobile communications. Wireless bandwidth is exponentially increasing, and there is a need to process all this data. Further, the wireless spectrum is both constrained and limited, and efficient use of this spectrum is needed.

Beamforming has attracted considerable interest with wide-ranging applications from radar, communication, microphone, and sensing applications. We are attracted to using beamforming to solve the wireless communication problems outlined previously. Specifically, we are interested in scenarios with a dynamically noisy interfering environment that require adaptive beamformers. By controlling the signal amplitudes and delays from each antenna element, the whole array can act in unison to steer the beam pattern [1]. Beamformers can continuously adjust their beam patterns and provide physical layer security by canceling dynamically changing interference.

Conventional RF beamformers rely on electrical phase shifters that restrict operation to the narrowband. Phase shifters notoriously suffer from beam squint problems. A beamformer’s beam pointing direction changes with signal frequency, limiting RF systems to narrowband [1]. A wide bandwidth system is necessary to ensure squint-free operation and uniformity of

the beampattern across wide frequencies. Photonic beamformers are attractive in that they inherently offer instantaneously wide bandwidth. The use of an optical system offers the advantages of reduced size, weight, power, low transmission loss, and immunity to electromagnetic interference.

Considerable research has been conducted in the field of photonic wideband beamforming [2]–[6]. True-time delay (TTD) beamformers are popular, and several methods have been proposed for TTD, including using fiber grating prisms [2], fiber-optic delay lines [3], dispersive fiber prisms [4], cross-gain modulation in SOAs [5], and integrated optical ring resonators [6]. Unfortunately, TTD beamformers are not suitable for adaptive beamformers, as they lack speed and precision. They are either discretely tunable with low resolution or are widely tunable but slow. Moreover, TTD beamformers lack any control in the frequency domain—they are only used as spatial processors.

Instead of TTD, several beamformers pair a transversal optical filter with each antenna in order to obtain spatiotemporal processing ability [7], [8]. However, neither architecture can be scaled to large arrays and are prohibitively expensive: The number of lasers required is linear with the number of antennas.

In this paper, we propose implementing a novel adaptive spatiotemporal broadband beamformer using discrete optics that is highly scalable across hundreds of antennas. The beamformer has been specifically designed for an application in a nonstationary, interfering environment. The adaptive algorithm that we introduce is loosely based on an algorithm proposed in the aviation field called guided accelerated random search (GARS) [9], but is new and tailored to our specific scenario and beamformer.

Our optical architecture offers the distinct advantage of scalability, as needed for practical systems with multiple antennas and taps, by using a novel single-mode to multimode (SM-MM) combiner. By eliminating coherent effects with this SM-MM combiner, our system uses the same fixed set of optical wavelengths for each antenna in the system. This allows us to save both space and cost, as we are able to use the same set of laser arrays for each and every antenna.

A theoretical beamformer was previously introduced by the authors in [10], but it is fully implemented and experimentally verified here. While a proof-of-concept adaptive wideband beamformer has been presented by [11], this is the first paper, to the authors’ knowledge, that a complete adaptive photonic beamformer system has been experimentally implemented. Most literature is focused on either simulating an adaptive algorithm or creating a photonic beamformer. However, pairing them is not trivial, and this paper marries the two.

Manuscript received January 8, 2014; revised February 25, 2014; accepted February 27, 2014. Date of publication March 3, 2014; date of current version September 1, 2014.

J. Chang and P. R. Prucnal are with the Lightwave Communication Research Laboratory, Princeton University, Princeton, NJ 08550 USA (e-mail: jcfive@princeton.edu; prucnal@princeton.edu).

J. Meister is with the IDA Center for Computer Sciences (CCS), Bowie, MD 20721 USA (e-mail: jemeist@super.org).

Color versions of one or more of the figures in this paper are available online at <http://ieeexplore.ieee.org>.

Digital Object Identifier 10.1109/JLT.2014.2309691

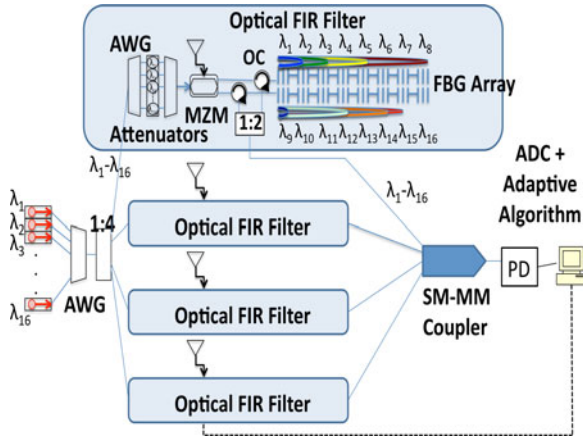


Fig. 1. Architecture for photonic beamformer.

## II. SYSTEM ARCHITECTURE OVERVIEW

In this section, we will introduce the optical architecture for our photonic beamformer and will describe the potential scalability of the system. The objective of a beamformer is to maximize the signal-to-noise ratio (SNR) through the suppression of noise and interfering signals by acting as a spatial filter. Temporal and frequency filtering capabilities can be achieved with finite impulse response filters (FIR) [12].

The response for a broadband beamformer is given by

$$P(\omega, \theta, \phi) = \sum_{m=0}^{M-1} \sum_{n=0}^{N-1} w_{m,n} e^{-j\omega(nT - \tau_m(\theta, \phi))} \quad (1)$$

where  $w_{m,n}$  represents the weight for the  $n$ th tap, delayed by an amount  $nT$ , of the filter corresponding to the  $m$ th antenna, and  $\tau_m$  is the time delay due to the array geometry.

We replicate equation (1) by using discrete optical components shown in Fig. 1. Our architecture utilizes four antennas, each with an eight-tap optical FIR filter. The beam pattern is steered by changing the weights of the FIR filters. The processed outputs of the antennas are summed using a special SM-MM optical combiner. The architecture is a blind adaptive approach, in that the beamformer and the adaptive algorithm only have access to the output of the system. This requires only a single conversion to RF (at the output), whereas traditional systems require an analog-to-digital card (ADC) for each antenna element, which is impractical for large antenna systems.

The beamformer is driven by two eight-channel distributed feedback (DFB) laser arrays. The 16 lasers ( $\lambda_1 = 1538.98$  nm to  $\lambda_{16} = 1563.05$  nm multiplexed with 200 GHz spacing) are combined using an arrayed-waveguide grating multiplexer (AWG mux), optically amplified using an EDFA, and split by a 1:4 passive splitter for distribution to four parallel optical FIR filters.

Our system consists of four parallel and identical optical FIR filters. One full filter is shown in Fig. 1 with block diagrams representing the other three. For each filter, the first set of wavelengths  $\lambda_{1-8}$  corresponds to the positive coefficients. The second set of wavelengths  $\lambda_{9-16}$  corresponds to the negative coefficients. An AWG demultiplexer is used to split the input to

each filter into sixteen parallel fibers, each containing a single wavelength. A thermal-optic attenuator array weights each coefficient. The attenuators are controlled by a voltage source have a response time of 10  $\mu$ s per 0.1 dB and a 30 dB range. The coefficients are combined using another AWG mux. The RF signal to be processed by the FIR filter is modulated onto the optical carrier using a  $1 \times 2$  dual output electro-optical Mach-Zehnder modulator (MZM) with phased-inversed dual outputs. The modulated signals of the outputs are biased at the inverse,  $\pi$ -shifted, portions of the modulator transfer function [13]. The modulated signals at the outputs are complimentary and are  $\pi$ -shifted out-of-phase so that they destructively interfere when combined. We use this complimentary output to implement negative coefficients. Both outputs have equal insertion losses of 3.7 dB.

The complimentary outputs are launched to fiber Bragg grating (FBG) arrays that only reflect and delay the wavelengths assigned to the respective coefficients, via an optical circulator (OC). Delays are created by forcing the coefficients to propagate along the FBG until reflected by a wavelength-specific grating. The coefficients encounter FBGs with the same delays, but correspond to different wavelengths. Each delay has a positive and negative coefficient tap, and the attenuator is used to disable one of them. In this way, our 16-wavelength filter provides eight positive/negative taps with 200 ps delays. The signals exit the FBGs and are combined with a 2:1 coupler to form the output of each filter.

To complete the beamformer, the outputs of the four parallel filters are combined using a SM-MM optical combiner, and then, detected by a multimode photodetector (PD). The electrical output is then converted using an ADC and processed by our adaptive algorithm on a computer.

The novelty of our architecture is in the use of the SM-MM combiner. Our main advantage is the scalability that allows the same set of 16 wavelengths to be used for each antenna. Typically, beat noise from coherent optical summing will occur when signals of the same optical wavelength are combined. Without the use of SM-MM combiner the architecture would require 16 lasers for each antenna, linearly increasing with each antenna. To “recycle” the same wavelengths, the SM-MM combiner couples signals from several individual single-mode fibers to distinct modes inside a multimode fiber. The multimode photodetector detects the total power from all of the individual inputs without optical interference and is phase-insensitive. In-depth information and experimental data demonstrating operation can be found in [14].

The architecture scales by simply adding optical splitters and amplifiers up to the limit imposed by the amplified spontaneous emission (ASE) of the amplifiers, as shown in Fig. 1. The attenuators do not limit the scalability of the architecture, nor does the addition of FBGs. An 100  $\mu$ m multimode fiber can accept up to 113 inputs or antennas [14]. Each optical FIR filter has an optical loss of around 24 dB. We are able to easily scale the system to at least 32 antennas without amplifying the system [10].

The number of FIR filter taps limits the frequency resolution of the system. Typical DSP filters have at least over 100 taps to have good resolution. An eight tap optical system, while broadband, lacks this fine resolution in frequency filtering.

Further, conventional beamformers are limited by the resolution and range of the delay lines. Optical taps are not limited by overall range of the delays, since a piece of optical fiber containing an FBG array is used to produce delays—they can be as long as necessary without adding additional bulk or loss to the system. Resolution of tap spacing is generally not a concern, as 100 ps delays can be easily produced corresponding a bandwidth of 10 GHz.

The overall RF performance of the photonic beamformer is very good and is comparable to similar optical architectures [15]. The total link loss is 19 dB, noise figure is 43 dB, and the SFDR is 89 dBm/ Hz.

The architecture outlined previously is used as a receiver but can easily be reconfigured to be a transmit array. An RF data source that is split equally between each of the optical FIR filters should replace the antennas in Fig. 1 and will be the input RF signal to the transmit array. Individual PDs should be placed at the output of each optical FIR filter (one for each antenna) and will convert the processed optical signal to the RF domain. By placing an antenna at the output of each PD, the architecture can be converted to a transmitter array, removing the SM-MM combiner from the system.

### III. INTRODUCTION TO GARS

Adaptive antenna arrays (beamformers) and the algorithms controlling their convergence have been studied extensively in literature [12], [16]. Widrow's seminal least-mean squares (LMS) algorithm was introduced in 1967, but research before and after have extensively focused on improving the reception of antenna sensor arrays by preserving a desired signal in the presence of interfering signals. Many methods for adaptive beamformers have been perfected over the years, including gradient-based algorithms, such as the LMS and Howells–Applebaum adaptive processor, direct matrix inversion of the signal environment, recursive methods, such as the least squares error processor and Kalman filtering, and cascade preprocessors, such as the Gram–Schmidt orthogonalization preprocessor [16]. While these algorithms can converge extremely quickly, they can become very complicated to implement with electronic hardware, requiring an exponential amount of correlators and ADCs (such as recursive methods and cascade preprocessors) or require a heavy computational load (such direct matrix inversion).

Like our photonic beamformer, we would like to introduce an algorithm that is computationally simple, cost-effective, and scales easily to a large number of antennas. We focus on a “blind” adaptive approach, which requires a single electronic ADC card to read the output of the entire beamformer, as shown in Fig. 1. We are unable to access the input signal to our antenna array and only have access to the processed output, giving the “blind” adjective to our approach. This severely limits the types of adaptive algorithms to use, as almost all algorithms in literature require the use of the input signal [16].

However, this type of “blind” approach offers the advantages of simplicity—for both the hardware (only one ADC is required) and computation (no matrix techniques need to be used). Moreover, established algorithms in literature rely heavily on the use

of training signals or mathematically knowing the signal of interest ( $d(t)$  in literature), which can be especially impractical in real-world situations.

We experimentally implement an adaptive random search algorithm nominally based on a search algorithm used in avionics called the GARS [9]. We keep the name of the method introduced by Barron, but only use it as a rough template and this paper's implementation is novel and unique to the authors'. We reworked Barron's method to suit our beamforming application and modified the weight space (from a two parameter problem to a 32-D space), its use, and its method of control and perturbation. We also measured the performance of the algorithm in a completely different way.

The algorithm consists of two stages: a random search stage and an accelerative “stepping” phase, in which weights are perturbed at an accelerated pace. As the algorithm progresses, it switches between the two stages depending on the performance of the array. We start with some arbitrary initial weight vector,  $w_0$ , measure beamformer performance, and store it as  $C^*$ . The algorithm starts off in the random phase, and the beamformer weights are perturbed ( $\Delta w$ ) according to a Gaussian probability density function with zero mean and standard deviation

$$\sigma^2 = K_1 + K_2 C^* \quad (2)$$

where  $C^*$  is the best performance value measured so far.  $K_1$  and  $K_2$  are design parameters, chosen so that the best convergence rate can be achieved. As a general rule, they are chosen so that the perturbation is large in the first few iterations of the algorithm (so that useful information can be gathered initially) and is small in the latter stages of the algorithm when optimum performance is close to being realized (so that the search is less noisy and fine-tuned). The next set of weights, iteration  $n+1$ , is generated by

$$w(n+1) = w(n) + \Delta w(n) \quad (3)$$

and performance is measured and recorded. If there is no improvement in the beamformer performance, the random phase is repeated again and a different set of random weights,  $w(n+2)$ , is generated from the same set of original weights,  $w(n)$ .

If there is an improvement, random phase reveals a direction of improvement, and the algorithm enters its accelerative stepping phase. A successful step is followed by another step with twice the magnitude in the same direction ( $\Delta w(n)$ ), and convergence is “accelerated” by continuing to move in the same direction with twice the previous step size. Step size is doubled with each iteration until there is drop in performance; once this happens, the algorithm repeats and reenters the random stage, with a more focused, smaller random step size since  $C^*$  has now improved.

One of the unique aspects of the GARS algorithm is the changing magnitude of the step size with performance. LMS, and many other algorithms, suffers from performance misadjustment when step size is chosen too small or large [12]. GARS avoids this by shrinking the weight space with performance—or by searching widely in the beginning when the weight space is not known, and reducing step size to the vicinity of the optimum as performance improves. The other unique aspect of GARS is

the accelerated doubling of step size with improvement, which leverages information learned of the weight space during the random search stage. This algorithm can be summarized as “smart acceleration”—go in a direction confidently when you know performance will increase otherwise gather information until you are confident.

Conventional algorithms previously introduced can suffer from dimensionality and modality of the search problem and weight environment; computational complexity and convergence rate can severely degrade with nonunimodal performance surfaces [9], [16]. Moreover, most algorithms rely on a good “initial” guess (one that is close to the optimum already) or having the beamformer presteered already [9], [12], [16]. GARS requires neither a good initial guess nor a unimodal problem. Its computational complexity is extremely simple, regardless of the problem or weight space.

The greatest advantage of the GARS algorithm is its versatility. Astute readers will notice that “beamformer performance” has been deliberately vague. Whereas, conventional adaptive algorithms are very specific to their required inputs or performance measures [12], [16], GARS can use any cost function to measure the performance [9]. For instance, max peak power, average power, minimum power, or discrete Fourier transform (DFT) of the beamformer output can all be used. A least-squares calculation between a measured signal and projected/ expected signal could even be used. GARS is not even limited to finding the minimum or maximum as both measures can be used. GARS versatility and simplicity allows it to be a practical adaptive algorithm that can be used across many fields and situations.

#### IV. EXPERIMENTAL RESULTS AND DISCUSSION

In this section, we experimentally demonstrate the interference cancellation abilities of our adaptive photonic beamformer. Tap spacing of the FIR filters was  $T = 200$  ps. The antenna array was arranged linearly with a spacing of  $d = 0.1$  m. Two signals both with 0 dBm of power, one interferer and one signal of interest (SOI), were generated by an RF signal generator separated by 15–20 ft away from the antenna array. The SOI was AM modulated with 25 kHz side band. Signals in the 900 MHz and 2.4 GHz bands were generated to mimic the GSM and WiFi bands.

Weights ranged from  $-768$  to  $768$ . The weights were used to control the voltage of the optical attenuators, and the 30 dB of range was split linearly. We used an initial weight vector of 614, or 80% of the full power, for each tap. This provided the beamformer with enough optical power for reception, but proved to be quite far from an optimal solution.

In our “blind” approach, we assume that we do not know anything about the desired signal, except for its frequency, rendering conventional algorithms useless. The cost function we chose in our case was to calculate power divided by the DFT of the outputted signal. The DFT is the cross-correlation between the output signal and frequency of the SOI and acts like a matched filter for the frequency of interest. By minimizing this ratio, we want to minimize total power while retaining some

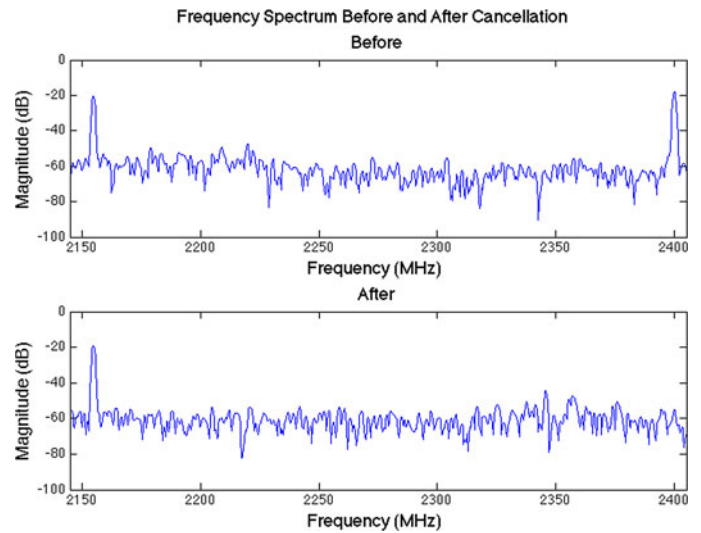


Fig. 2. Spectrum before (top) and after (bottom) for interferer (2.4 GHz) and SOI (2.15 GHz)  $60^\circ$  apart.

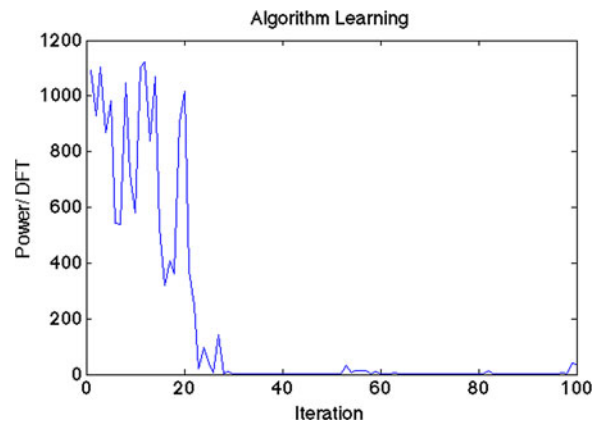


Fig. 3. Learning curve for interferer (2.4 GHz) and SOI (2.15 GHz)  $60^\circ$  apart.

signal at the frequency of the SOI. The idea is to be able to cancel interference but preserve the SOI.

We first show the performance of the GARS algorithm when the SOI, at 2.15 GHz, and the interference, at 2.4 GHz, are spaced  $60^\circ$  apart. Fig. 2 shows the RF spectrum analyzer (SA) measurements of the PD of the photonic beamformer before (top) and after (bottom) convergence. We are able to cancel the interference by a total 37.092 dB while retaining the SOI.

The learning curve for this scenario is shown below in Fig. 3, and the distribution of the filter weights is shown below in Fig. 4. The learning curve shows our power/ DFT cost function, calculated directly from our ADC card. Initially there is a lot of noise as the GARS enters its random stage, but one sees nearly full convergence by  $\sim 30$  iterations. Convergence happens quite quickly (within a couple of iterations), as expected with the accelerated doubling of the step size.

We see that the weights initially traverse widely among the weight space, but as performance increases and steady-state is reached, the weights reach steady state as well. We can see the dependence of the weights on the performance of the cost function, as when noise is encountered on the learning curve

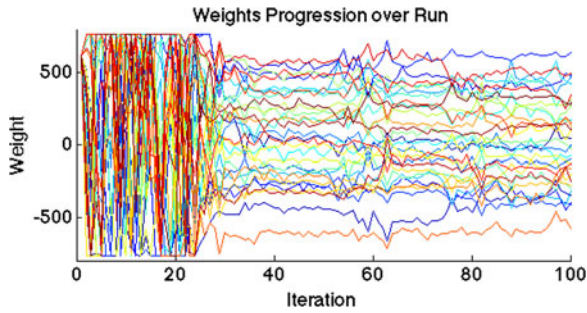


Fig. 4. Weights versus iteration for interferer (2.4 GHz) and SOI (2.15 GHz) 60° apart.

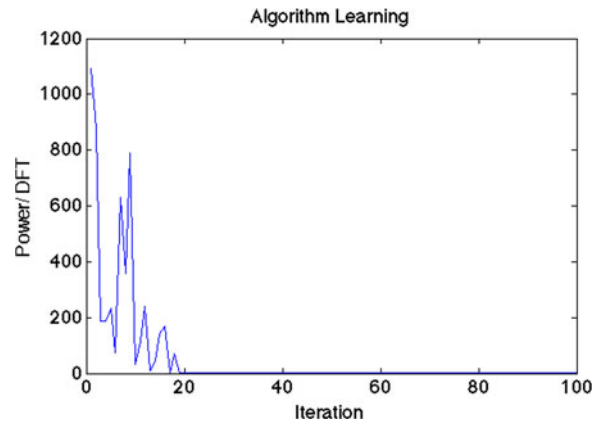


Fig. 6. Learning curve for interferer (2.4 GHz) and SOI (2.3 GHz) 60° apart.

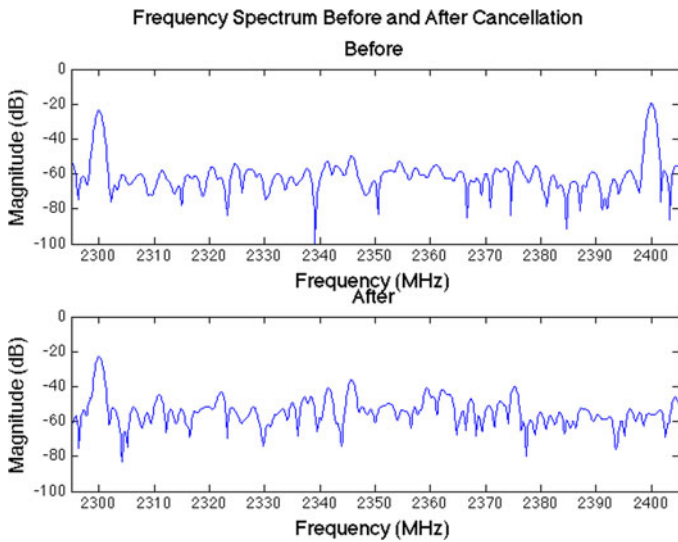


Fig. 5. Spectrum before (top) and after (bottom) for interferer (2.4 GHz) and SOI (2.3 GHz) 60° apart.

(as a bump), there is a similar bump and increase of weight perturbation.

To show the reconfigurability of the beamformer with regards to frequency, we show a similar scenario when the SOI and interferer are now closer, at 100 MHz apart. The SA shows spectrum of the beamformer before and after cancellation in Fig. 5, and a total cancellation of 36.216 dB is achieved. The learning curve is shown in Fig. 6, and we see that we can converge ~20 iterations. The weights versus iterations is shown in Fig. 7 and mimic the learning curve.

To show the broadband nature of our beamformer, we show another scenario in which the interferer (915 MHz) is in the GSM band. The SOI (765 MHz) and the interferer are 30° apart. We are able to achieve a cancellation of 33.947 dB from the SA measurements in Fig. 8. Figs. 9 and 10 show the learning curve and weights versus iteration curve for this scenario. Convergence is achieved ~45 iterations. There is a series of small peaks on the learning curve from 20–40 iterations, and this is mirrored in the widening of the weight step size perturbations in Fig. 10.

Fig. 11 shows the calculated beampattern based on weights calculated during the adaptive run. Fig. 11 shows a null at -30° and 915 MHz and a peak at 0° and 765 MHz as expected.

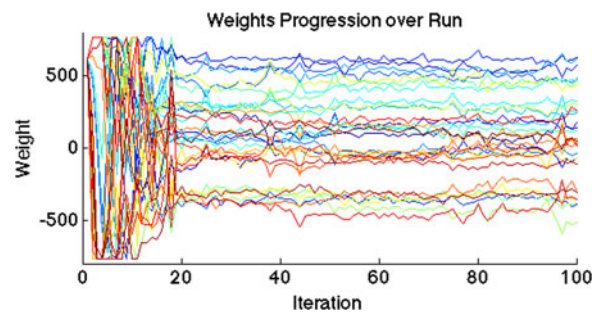


Fig. 7. Weights versus iteration for interferer (2.4 GHz) and SOI (2.3 GHz) 60° apart.

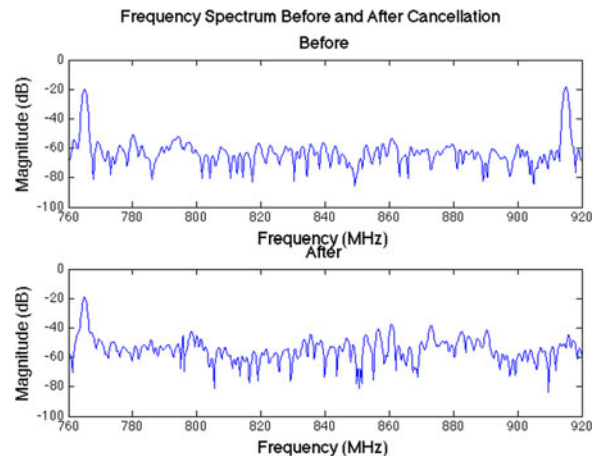


Fig. 8. Spectrum before (top) and after (bottom) for interferer (915 MHz) and SOI (765 MHz) 30° apart.

To show the reconfigurability of the beamformer with regards to spatial filtering, we show a scenario with the same interference and SOI as before, but spaced 10° apart. We are able to achieve a cancellation of 34.895 while preserving the SOI, shown in Fig. 12. Figs. 13 and 14 show the learning curve and weights versus iteration curve for this scenario. While initially very noisy, convergence is achieved ~25 iterations.

Finally, to show versatility of the GARS algorithm, we decide to maximize the DFT as the new cost function. We have only a SOI at 915 MHz and broadside to the antenna array. Starting

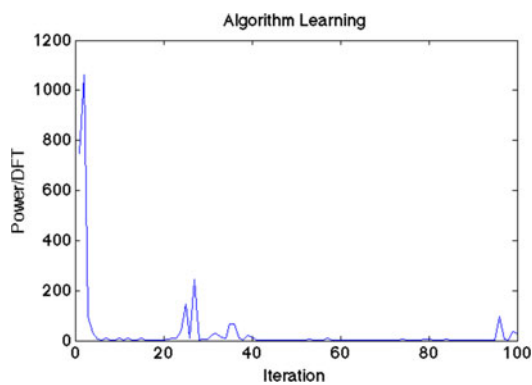


Fig. 9. Learning curve for interferer (915 MHz) and SOI (765 MHz) 30° apart.

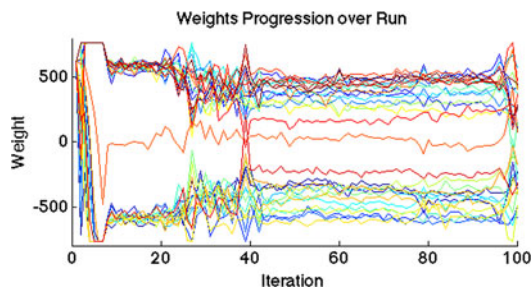


Fig. 10. Weights versus iteration for interferer (915 MHz) and SOI (765 MHz) 30° apart.

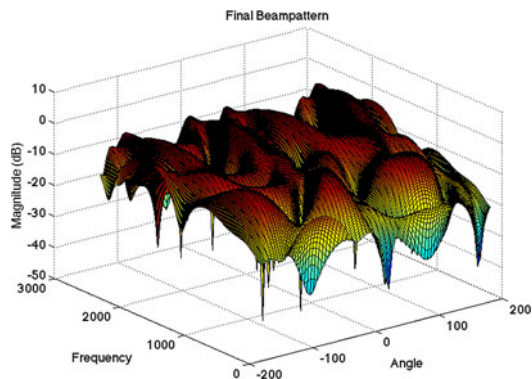


Fig. 11. Final beam pattern for interferer (915 MHz) and SOI (765 MHz) 30° apart.

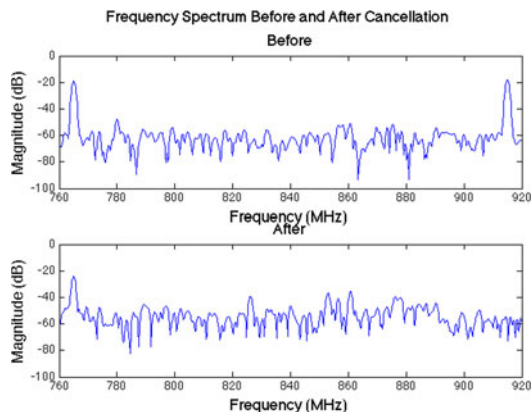


Fig. 12. Spectrum before (top) and after (bottom) for interferer (915 MHz) and SOI (765 MHz) 10° apart.

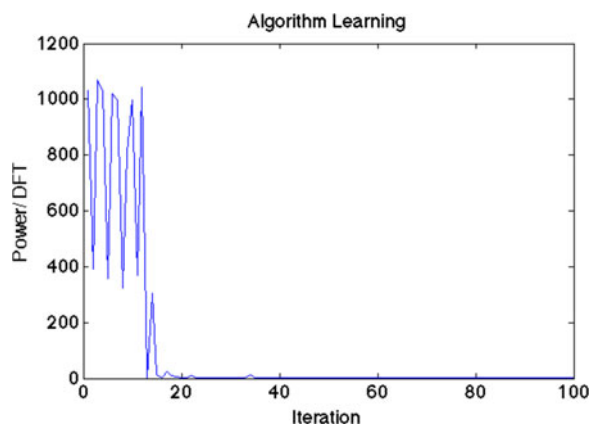


Fig. 13. Learning curve for interferer (915 MHz) and SOI (765 MHz) 10° apart.

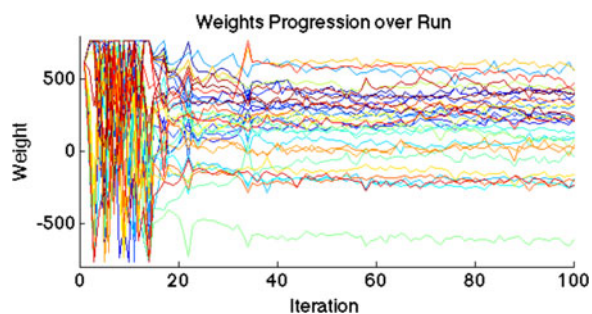


Fig. 14. Weights versus iteration for interferer (915 MHz) and SOI (765 MHz) 10° apart.

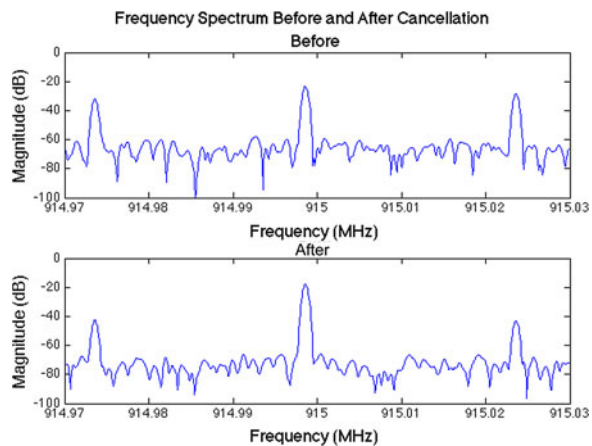


Fig. 15. Spectrum before (top) and after (bottom) for an SOI (765 MHz).

weights were set to 384 or 50% of total power. We were able to increase the power of an AM modulated SOI, show below in Fig. 15. The signal has been spatially aligned by the beamformer to add coherently and give a 5.359 dB increase in power.

The performance shown previously shows substantial cancellation over a wide variety of different frequency bands, different interferers and SOIs, and different angles. Convergence was achieved extremely quickly and under 50 iterations for all cases. These results show not only the instantaneous bandwidth and cancellation ability of the photonic beamformer, but the validity and usefulness of the GARS algorithm as well.

An array with  $N$  antennas is able to produce nulls for  $N-1$  interferers [16]. Thus, our system is capable cancelling up to three interferers, but more nulls can be produced by simply scaling the number of antennas.

## V. CONCLUSION

In this paper, we have introduced a novel photonic beamformer for the adaptive cancellation of interference in the presence of a SOI. The use of a SM-MM combiner gives the photonic architecture great scalability across many antennas. We have also presented an extremely simple and versatile adaptive search algorithm, GARS, to be used in cases of a “blind” environment. We have experimentally demonstrated a maximum cancellation of  $\sim 37$  dB with a convergence time of under 50 iterations.

Integration of the photonic components into an integrated beamformer has been investigated very recently [17], [18]. Our next step is to investigate a scalable integrated photonic beamformer that can be electronically controlled by the GARS algorithm.

## REFERENCES

- [1] J. Yao, “A tutorial on microwave photonics,” *IEEE Photon. Soc. News*, vol. 26, no. 3, pp. 5–11, Jun. 2012.
- [2] H. Zmuda, R. A. Soref, P. Payson, and S. Johns, “Photonic beamformer for phased array antennas using a fiber grating prism,” *IEEE Photon. Technol. Lett.*, vol. 9, no. 2, pp. 241–243, Feb. 1997.
- [3] L. Jofre, C. Stoltidou, S. Blanch, T. Mengual, B. Vidal, J. Marti, I. McKenzie, and J. M. Del Cura, “Optically beamformed wideband array performance,” *IEEE Trans. Antennas Propag.*, vol. 56, no. 6, pp. 1594–1604, Jun. 2008.
- [4] M. Y. Frankel, P. J. Matthews, and R. D. Esman, “Two-dimensional fiber-optic control of a true time-steered array transmitter,” *IEEE Trans. Microw. Theory Tech.*, vol. 44, no. 12, pp. 2696–2702, Dec. 1996.
- [5] X. Weiqi and J. Mork, “Microwave photonic true time delay based on cross gain modulation in semiconductor optical amplifiers,” in *Proc. OptoElectronics Commun. Conf.*, 2010, pp. 202–203.
- [6] M. Burla, M. R. H. Khan, D. A. I. Marpaung, L. Zhuang, C. G. H. Roeloffzen, A. Leinse, M. Hoekman, and R. Heideman, “Separate carrier tuning scheme for integrated optical delay lines in photonic beamformers,” in *Proc. Int. Top. Meet. Microw. Photon.*, 2011, pp. 65–68.
- [7] H. Zmuda and E. N. Toughlian, “Broadband nulling for conformal phased array antennas using photonic processing,” in *Proc. Int. Top. Meet. Microw. Photon.*, 2000, pp. 17–19.
- [8] N. A. Riza, “High speed multi-beamforming for wideband phased arrays,” in *Proc. Int. Top. Meet. Microw. Photon.*, 2003, pp. 405–409.
- [9] R. L. Barron, “Inference of vehicle and atmosphere parameters from free-flight motions,” *AIAA J. Spacecraft Rockets*, vol. 6, no. 6, pp. 641–648, Jun. 1969.
- [10] J. Chang, M. P. Fok, R. M. Corey, J. Meister, and P. R. Prucnal, “Highly scalable adaptive photonic beamformer using a single mode to multimode optical combiner,” *IEEE Microw. Wireless Comp. Lett.*, vol. 23, no. 10, pp. 563–565, Oct. 2013.
- [11] X. Guan, H. Zmuda, L. Jian, D. Lin, and M. Sheplak, “Hardware implementation of wideband time domain Robust Capon Beamforming,” in *Proc. IEEE Int. Symp. Antennas Propag.*, Jul. 2011, pp. 2849–2852.
- [12] B. Widrow, P. E. Mantey, L. J. Griffiths, and B. B. Goode, “Adaptive antenna systems,” *Proc. IEEE*, vol. 55, no. 12, pp. 2143–2159, Dec. 1967.
- [13] D. B. Hunter, “Incoherent bipolar tap microwave photonic filter based on balanced bridge electro-optic modulator,” *Electron. Lett.*, vol. 40, no. 14, pp. 856–857, 2004.
- [14] J. Chang, M. Fok, J. Meister, and P. Prucnal, “A single source microwave photonic filter using a novel single-mode fiber to multimode fiber coupling technique,” *Opt. Exp.*, vol. 21, pp. 5585–5593, 2013.
- [15] M. Lu, M. Chang, Y. Deng, and P. Prucnal, “Performance comparison of optical interference cancellation system architectures,” *Appl. Opt.*, vol. 52, pp. 2484–2493, 2013.
- [16] R. Monzingo, R. L. Haupt, and T. W. Miller, *Introduction to Adaptive Arrays*, 2nd ed. Raleigh, NC, U S: Scitech Publishing, Inc., p. 201.
- [17] D. Marpaung, Z. Leimeng, M. Burla, C. Roeloffzen, B. Noharet, Q. Wang, W. P. Beeker, A. Leinse, and R. Heideman, “Photonic integration and components development for a Ku-band phased array antenna system,” in *Proc. Int. Top. Meet. Microw. Photon. Conf.*, Oct. 2011, pp. 458–461.
- [18] L. Zhuang, D. Marpaung, M. Burla, C. Roeloffzen, W. Beeker, A. Leinse, and P. Van Dijk, “Low-loss and programmable integrated photonic beamformer for electronically-steered broadband phased array antennas,” in *Proc. Photon. Conf.*, 2011, pp. 137–138.

**John Chang** (S’10–M’12) received the B.S.E and M.A. degrees from Princeton University, Princeton, NJ, in 2010 and 2012, respectively, where he is currently working toward the Ph.D. degree in electrical engineering with an anticipated graduation date in 2014.

His research focuses on RF photonics and various types of technologies of optical signal processing techniques.

**James Meister** (S’74–M’77–F’79) received the B.A. degree in mathematics from the University of Connecticut, Storrs, CT, USA, in 1974 and the M.A and Ph.D. degrees in mathematics from Cornell University, Ithaca, NY, USA, in 1977 and 1979, respectively.

He was a Principal Engineer at Raytheon from 1980 to 1987 working on various advanced development Electronic Warfare programs. From 1987 to 1999, he was a Principal Scientist at DRS Technologies, where his interests were in acoustic signal processing algorithms and modeling of sonar signals. Since 1999, he has been a Research Staff Member at the Institute for Defense Analyses Center for Computing Sciences, involved in many RF and signal processing programs.

**Paul R. Prucnal** (S’75–M’79–SM’90–F’09) received the A.B. degree from Bowdoin College, Brunswick, ME, USA, and the M.S., M.Phil., and Ph.D. degrees from Columbia University, New York, NY, USA.

He was a Faculty Member with Columbia University until 1988, when he joined Princeton University, Princeton, NJ, USA, as a Professor of electrical engineering. From 1990 to 1992, he served as the Founding Director of Princeton’s Center for Photonics and Optoelectronic Materials. He has also held positions as a Visiting Professor with the University of Tokyo and University of Parma. He is the inventor of the “Terahertz Optical Asymmetric Demultiplexer,” an ultra-fast all-optical switch, and is credited with doing seminal research in the areas of all-optical networks and photonic switching, including the first demonstrations of optical code-division and optical time-division multiaccess networks in the mid-1980s. With DARPA support in the 1990s, his group was the first to demonstrate a 100-Gbit/s photonic packet switching node and optical multiprocessor interconnect, which was nearly 100 times faster than any system with comparable functionality at that time. For the past several years, his research has focused again on optical CDMA as well as physical layer security in optical networks. He has authored or coauthored more than 200 journal papers and holds 17 patents.

Prof. Prucnal is a Fellow of the Optical Society of America (OSA). He was general chair of the OSA Topic Meeting on Photonics in Switching in 1999 and a received the Rudolf Kingslake Medal from SPIE. In 2005, he was received a Princeton University Engineering Council Award for Excellence in Teaching and, in 2006, and the Graduate Mentoring Award in Engineering at Princeton. He is currently an Area Editor of the IEEE Transactions on Communications for Optical Networks.